analytical chemistry

Article

pubs.acs.org/ac

Development of an Oligopeptide Functionalized Surface Plasmon Resonance Biosensor for Online Detection of Glyphosate

Xiaokang Ding and Kun-Lin Yang*

Department of Chemical and Biomolecular Engineering, National University of Singapore, 4 Engineering Drive 4, Singapore, 117576

Supporting Information

ABSTRACT: We report a surface plasmon resonance (SPR) biosensor for online detection of glyphosate. The surface of the sensing element is decorated with an oligopeptide, TPFDLRPSSDTR, which is identified by using phage display library. This oligopeptide shows high binding specificity for glyphosate (K_D = 8.6 μM), probably because of the presence of R and D in the oligopeptide. To detect glyphosate in buffer solution, an SPR gold sensor chip is modified by using the oligopeptide with a surface density of 0.6 1/nm^2. The sensitivity of this oligopeptide-functionalized SPR biosensor is 1.02 RU/μM whereas the limit of detection (LOD) is 0.58 μM. This oligopeptide functionalized SPR biosensor also shows good specificity against other analytes such as glycine, thiacloprid, and imidacloprid.

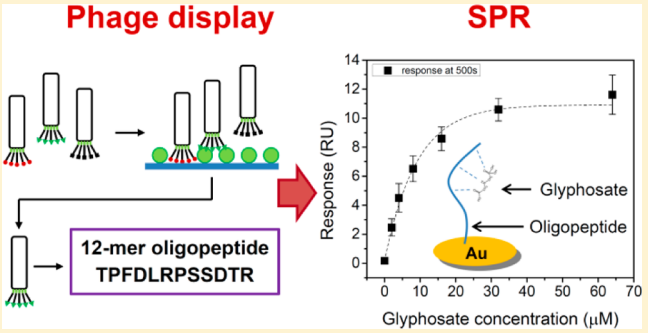

Glyphosate (*N*-(phosphonomethyl)glycine) is a herbicide that is used to kill weeds in farms, parks, and gardens.[1] Glyphosate is toxic to plants because it can interfere with the synthesis of aromatic amino acids such as phenylalanine, tyrosine, and tryptophan by inhibiting the enzyme activity of 5-enolpyruvylshikimate-3-phosphate synthase (EPSPS).[2] However, the widespread application of glyphosate has caused several problems. For example, residues of glyphosate in water may cause adverse effects on some aquatic plant species.[3,4] Recent studies also show that glyphosate is a potential endocrine disruptor.[5] Currently, the maximum residue levels (MRLs) of glyphosate in United States and Canada are 0.70 μg/mL (4.14 μM)[6] and 0.28 μg/mL (1.66 μM),[7] respectively. Therefore, monitoring of glyphosate in crops, fruits, vegetables, and drinking water has gained increasing importance.

Among numerous analytical methods, high-performance liquid chromatography (HPLC)[8,9] and gas chromatography–mass spectroscopy (GC/MS)[10,11] are widely used for the detection of glyphosate and its main metabolite, aminomethylphosphonic acid (AMPA). However, to achieve the required limit of detection, derivatization of glyphosate to incorporate chromophores or fluorophores is often needed.[12,13] Some methods, such as coulometric,[1,14] capillary electrophoresis,[15,16] amperometry,[17] and cyclic voltammetry,[18] do not require the derivatization step, but these methods usually do not have high sensitivity and specificity. On the other hand, enzyme-linked immunosorbent assay (ELISA) can be used to detect glyphosate with high specificity. For example, Clegg et al.[19] used a competitive ELISA for the detection and quantitation of glyphosate with a detection limit of 7.6 μg/mL. Similarly, Rubio et al.[20] described an ELISA for the detection of glyphosate after it was derivatized with acetic anhydride. This ELISA has a detection limit as low as 0.6 ng/mL. Both methods show good specificity toward a wide range of agrochemicals, and the cross-reactivity is less than 0.1%. However, a common problem in ELISA is the need to raise antibodies. Since glyphosate is a small molecule, it needs to be conjugated with bovine serum albumin (BSA) to form an immunogen which can elicit an immune response in animals. The production of antibodies is time-consuming and expensive, and the batch-to-batch variation is a concern. In additon, despite their good binding affinity and specificity, the antibodies are vulnerable to environmental factors, especially high temperature.[21]

Oligopeptide is a good candidate to replace antibodies in an immunoassay as a biomolecular receptor.[21,22] One important advantage for oligopeptides is that they are more stable and resistant to harsh environments.[23] Second, it is easier to synthesize oligopeptides with desired sequences for binding specific targets.[24] Previously, a large number of protein-binding oligopeptide sequences have been identified by using phage libraries. For example, Kim et al.[25] identified oligopeptides which bind to a cancer biomarker, tenascin C, by using a phage library, and the selected oligopeptide can specifically recognize tenascin C protein in mouse tissue. A phage library was also employed to identify oligopeptides which bind to inorganic materials, such as ZnS,[26] CdS,[27] ZnO,[28] and TiO_2,[29] and small organic molecules such as trinitrotoluene (TNT) and 2,4-dinitrotoluene (DNT).[30] For example, Jaworski et al.[30] identified two oligopeptides that can specifically bind to TNT and DNT from the phage library and demonstrated that the

Received: January 27, 2013
Accepted: May 15, 2013

   dx.doi.org/10.1021/ac400273g | *Anal. Chem.* XXXX, XXX, XXX–XXX

oligopeptides embedded in a hydrogel can selectively bind to DNT molecules in gas phase. Cerruti et al.[31] demonstrated that the oligopeptides can be used as a sensitive layer for real-time detection of TNT in water using a quartz crystal microbalance (QCM). Recently, we have developed a surface plasmon resonance (SPR) biosensor for the detection of two closely related neonicotinoid molecules, thiacloprid and imidacloprid.[32] The main advantage of a phage library is that phages can be used to identify target-binding oligopeptides through screening. However, in the studies mentioned above, insoluble solids were used as binding targets during the screening procedure. Therefore, the original phage library is not suitable for molecules with high solubility such as thiamethoxam (TMX) or glyphosate. To overcome this problem, Cho et al.[33] reported a phage display in which saturated TMX solution was used to prevent the dissolution of TMX crystals. In another study, Cui et al.[34] immobilized octyltrimethoxysilane on a silicon wafer as the binding target. This study showed that M13 phage can recognize molecules immobilized on solid surface. They also introduced a "negative screening" method to eliminate those phages that bind to the substrate.

Because glyphosate is highly soluble in water (10.1 mg/mL in water at 20 °C), we modified the original phage library to overcome the high solubility issue. First of all, glyphosate was covalently immobilized on amine-functionalized glass beads through EDC/NHS chemistry. The glass beads were used as a solid support to prevent the loss of glyphosate during screening procedures. Oligopeptides, identified from the phage library, and their binding capabilities for glyphosate were characterized in detail. We also developed a biosensor using surface plasmon resonance (SPR) functionalized with the oligopeptides for online detection of glyphosate in buffer solution.

EXPERIMENTAL SECTION

Materials. Glass slides and dialysis membrane (MWCO: 1000 Da) were obtained from Fisher (U.S.A). Glyphosate, thiacloprid, imidacloprid, and fluorescein isothiocyanate isomer I (FITC) were purchased from Sigma (Singapore). Glycine, cysteine, methanol (HPLC grade), and dimethyl sulfoxide (DMSO) were purchased from Merck (Singapore). Glass beads (Supelco, d = 75 μm), *N*-(3-dimethylaminopropyl)-*N*′-ethylcarbodiimide hydrochloride (EDC), *N*-hydroxysulfosuccinimide sodium salt (Sulfo-NHS), Tween-20, (3-aminopropyl)-triethoxysilane (APES), sodium carbonate, agar, polyethylene glycol (PEG, MW = 8000 g/mol), and isopropyl β-D-thiogalactoside (IPTG) were purchased from Sigma (Singapore). Ph.D.-12 phage display library kit was purchased from New England Biolabs (U.S.A). Luria broth base was purchased from Invitrogen (Singapore). 5-Bromo-4-chloro-3-indolyl-β-D-galactoside (X-gal) was purchased from Duchefa (The Netherlands). Tris buffer (1M, pH 8.0), phosphate buffer saline (PBS buffer, 10X) and TE buffer (10 mM Tris-HCl pH 8.0, 1 mM EDTA) were purchased from First Base (Singapore). Oligopeptides (purity ≥95%) were synthesized by GenicBio (Shanghai, China). BIAcore gold sensor chip (uncoated), borate buffer (10 mM disodium tetraborate, pH 8.5, and 1 M NaCl), glycine-HCl (10 mM glycine-HCl, pH 2.0), HBS-EP buffer (0.01 M HEPES, pH 7.4, 0.15 M sodium chloride, 3 mM EDTA, and 0.005% v/v surfactant P20) were purchased from GE Healthcare (Singapore). Deionized water (18 MΩ cm) was obtained from a Millipore filtration system.

Surface Functionalization of Glass Beads. The schematic cartoon for the functionalization of glass beads is shown in Figure 1. First, glass beads were functionalized with (3-aminopropyl)triethoxysilane (APES). To clean the surface,

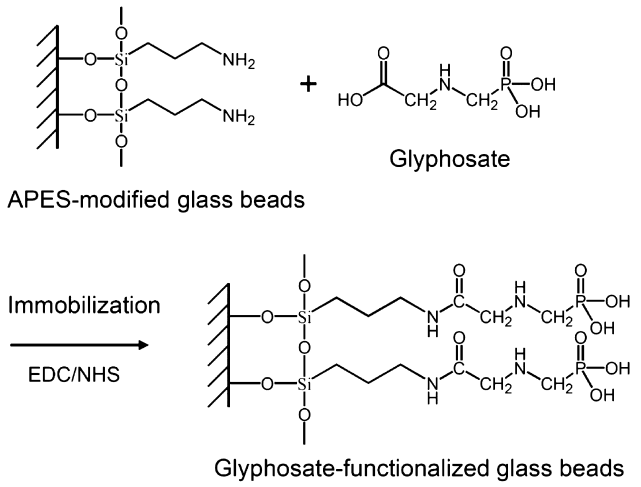

Figure 1. Schematic illustration for the immobilization of glyphosate on amine-modified glass beads by using EDC/NHS chemistry.

500 mg of the glass beads were immersed in a 5% Decon-90 solution (a commercially available detergent). After 2 h of constant shaking, the glass beads were sonicated in the solution for 15 min. After this, they were rinsed with DI water and sonicated for 15 min twice. Clean glass beads were then rinsed with methanol twice and dried at 50 °C overnight. To silanize the glass beads, 50 mg of the glass beads were incubated in 1 mL of aqueous solution containing 90.4 mM of triethoxysilan APES at 50 °C under gentle rocking. After 1 h, the solution was decanted, and the glass beads were washed thoroughly with DI water and methanol to remove residual silanes. The APES-coated glass beads were heated in a 100 °C vacuum oven for 15 min to allow the cross-linking of APES. To examine the surface density of amine groups, the APES-coated glass beads were incubated in sodium carbonate buffer (100 mM, pH 9.0) containing 10 μg/mL of FITC. After 1h, the glass beads were washed thoroughly with 0.1 wt % SDS solution and DI water to remove remaining FITC. To observe fluorescent images, 2 μL of water containing suspended glass beads was dispensed onto a piece of glass slide. Fluorescent images of all samples were observed with a fluorescence microscope (Eclipse E200, Nikon, Japan), which was equipped with an FITC/EGFP filter (USA). All images were captured by using a digital camera (ACT-2U, Nikon) mounted on top of the fluorescence microscope with exposure time of 1s. The fluorescent images were analyzed by using ImageJ (1.42Q) to obtain fluorescent intensity profiles. After that, glyphosate was immobilized on the amine-functionalized glass beads. First, 10 mg/mL of glyphosate was dissolved in 10 mM HEPES buffer (pH 7.0) containing 200 mM of EDC and 50 mM of Sulfo-NHS to activate carbonyl groups on glyphosate. After 10 min, 200 μL of the solution was mixed with 50 mg of APES-coated glass beads. After 1 h of reaction, the supernatant was decanted, and the glass beads were washed twice with 0.1 wt % SDS solution and DI water to remove nonreacted glyphosate. The glyphosate surface density was determined by using the fluorescent method as described above.

Phage Display. Figure 2 shows the phage display library screening employed in this study. Briefly, 10 μL of phage library (1×10^{13} pfu/mL, complexity 2.7×10^{9}) was added to 1.5 mL

dx.doi.org/10.1021/ac400273g | Anal. Chem. XXXX, XXX, XXX−XXX

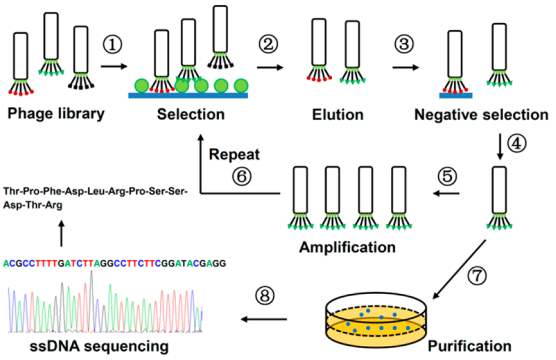

Figure 2. Schematic illustration of using the phage library for screening glyphosate-binding oligopeptides. (1) A phage library is incubated with glass beads functionalized with glyphosate, (2) the bound phages are eluted by lowering pH, (3) the phages are exposed to APES-coated glass beads for negative selection, (4) the phages are collected that do not bind to the glass beads, (5) the surviving phages are amplified, (6) the screening procedure is repeated with the amplified phage, (7) the phage colony is purified with plate titering, and (8) DNA is sequenced, and oligopeptide sequence is deduced from a codon table.

of 0.1% TBST buffer which contains 50 mM of Tris-HCl (pH 7.4), 150 mM NaCl, and 0.1% v/v of Tween-20. Then, this solution was mixed with 20 mg of glyphosate-coated glass beads and incubated for 30 min under vigorous shaking. After 30 min, the buffer solution was decanted, and the glass beads were washed with 1 mL of fresh 0.1% TBST buffer 10 times to remove nonspecific adsorbed phages. Bound phages were eluted with 1 mL of 0.2 M glycine-HCl (pH 2.2), 1 mg/mL of BSA, and the solution was collected and neutralized with 150 μL of 1 M Tris-HCl (pH 9.1). To exclude phages which bind to the glass beads, the eluted phages were mixed with 20 mg of APES-coated glass beads (negative screening). Subsequent steps of phage amplification, titering and DNA sequencing steps can be found in the manual of Ph.D-12 phage display kit.[35]

Phage Binding Analysis. We determined the strongest and most selective glyphosate-binding phages using single-phage binding assays. First, five single-phage colonies expressing different oligopeptides, including TPFDLRPSSDTR ($\mathbf{P_1}$), TDIRLRPLDKRI ($\mathbf{P_2}$), RLKPRSDIKPIR ($\mathbf{P_3}$), SDTPLIKRLDFP ($\mathbf{P_4}$), and RRSDLKPIRPLK ($\mathbf{P_5}$), were amplified to ~10^{12} pfu/mL by using *Escherichia coli* (ER2738). Then, 200 μL of the amplified phage solution, together with original phage library, was added to 20 mg of glyphosate-coated glass beads separately. After one round of screening, the bound phages were eluted from glyphosate-coated plates by 0.2 M glycine-HCl (pH 2.2), 1 mg/mL BSA solution, and then neutralized with 1 M Tris-HCl (pH 9.1). This eluted phage was titered on LB/IPTG/Xgal plates as described above, and the number of blue plaques was counted to determine the phage titer in plaque-forming units per mL (pfu/mL).

Surface Plasmon Resonance (SPR). Glyphosate-binding oligopeptide TPFDLRPSSDTRGGGC ($\mathbf{P_1}$-cys) and alanine-substituted control oligopeptide TPFALAPSSATAGGGC ($\mathbf{P_m}$-cys) were custom synthesized by GenicBio (Shanghai, China). GGGC was added to the carboxyl-terminus of the original sequence to provide a spacer and an anchoring point (through cysteine) for immobilization. To immobilize the oligopeptide on the SPR gold sensor chip, the oligopeptide was dissolved in immobilization buffer (10 mM disodium tetraborate and 1 M NaCl, pH 8.5) to a final concentration of 1.0 mg/mL. Then, the solution was injected into the flow cell of a sensor chip under a constant flow rate of 1 μL/min for 325 min. After immobilization, the sensor chip was rinsed with HBS-EP buffer for 30 min to remove unreacted oligopeptides. To avoid nonspecific adsorption of glyphosate, we blocked the sensor chip with 10 mM of cysteine. In the BIAcore SPR system, a response of 1000 RU corresponds to a change in surface density of about 1 ng/mm^2.[36] The surface density of oligopeptides on the SPR sensor chip surface was calculated on the basis of this number.

Next, HBS-EP buffer containing different concentrations of glyphosate were injected sequentially into a flow channel at a flow rate of 2 μL/min at the beginning of each cycle. Each cycle consists of a binding step for 3 min, a rinsing step with fresh HBS-EP buffer for 2.5 min, and a regeneration step with glycine-HCl solution (pH 2.0) for 1 min. To eliminate background signal, a reference flow channel (blocked with 10 mM of cysteine only) was subjected to the same binding cycle. Reported SPR sensorgram data are the difference between the test channel (immobilized with oligopeptide) and reference channel (only blocked with10 mM of cysteine). The final binding responses for different glyphosate concentrations are obtained from the SPR sensorgrams at 500 s.

RESULTS AND DISCUSSION

Immobilized Glyphosate on Glass Beads. To immobilize glyphosate on the surface of glass beads, the glass beads were first functionalized with APES. The surface density of amine groups at different APES concentrations was quantified by using fluorescence as shown in Figure 3A. We note that the

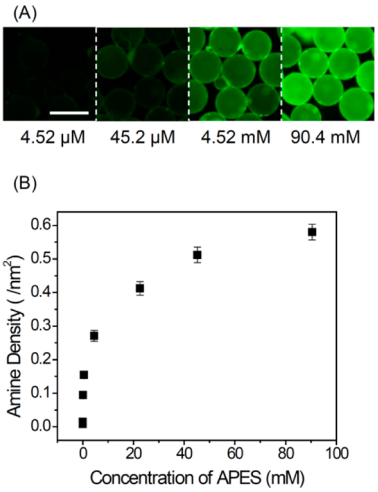

Figure 3. Determination of surface free amine density on the glass beads by using the fluorescence method. (A) Fluorescence images of the glass beads after silanization at different APES concentrations, as indicated in the numbers below. The scale bar is 100 μm. (B) Surface free amine density as a function of APES concentration.

fluorescence intensity of the glass beads increases with the increase of APES concentration. This is expected because a higher APES concentration can lead to a higher surface density of primary amine groups, which can react with FITC. Figure 3B shows the calculated surface density of amine groups as a function of APES concentration. When the APES concentration is 90.4 mM, the surface density of amine group reaches 0.58

dx.doi.org/10.1021/ac400273g | *Anal. Chem.* XXXX, XXX, XXX−XXX

(amine/nm^2) (see Supporting Information [SI]), which is smaller than the reported value (2.5 amine/nm^2).[37] This is probably because the surface density of the silanol group is lower (we did not activate the glass beads with strong acids/bases). From Figure 3B, we also noticed that the glass surface is saturated with the amine group when the APES concentration is 90.4 mM. To achieve the best result for glyphosate immobilization, we fixed the APES concentration at 90.4 mM in the following experiments.

Next, glyphosate was immobilized on the APES-coated glass beads by using NHS/EDC chemistry. To quantify the amount of glyphosate immobilized on the surface, we used fluorescence to determine the surface density of the free amine group before and after the immobilization. Then, the difference in free amine group before and after the reaction is taken as the amount of immobilized glyphosate on the surface. Figure 4A shows the

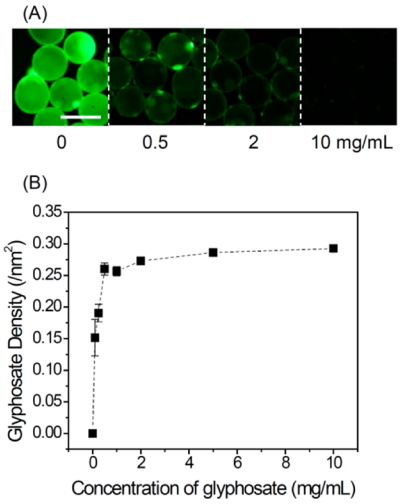

Figure 4. Determination of surface glyphosate density on the glass beads by using fluorescence method. (A) Fluorescence images of the glass beads after immobilization of glyphosate at different glyphosate concentrations, as indicated in the numbers below. Scale bar is 100 μm. (B) Surface glyphosate density as a function of glyphosate concentration.

fluorescence images of the glass beads after they react with glyphosate at various concentrations. We note that the fluorescence intensity generally decreases with increasing glyphosate concentration. However, when the glyphosate concentration is 10 mg/mL, no fluorescence is observed, indicating that all free amine groups are consumed during the reaction. Figure 4B shows the surface density of glyphosate as a function of glyphosate concentration used in the immobilization. We can see that the surface density of glyphosate increases when the glyphosate concentration is increased from 0 to 10 mg/mL. When the glyphosate concentration is 10 mg/mL, the surface is already saturated with glyphosate. Therefore, we used 10 mg/mL of glyphosate to obtain a full coverage of glyphosate on the surface in the following experiments.

Identification of the Glyphosate Binding Phage. To obtain glyphosate-binding oligopeptides, we employed glyphosate-decorated glass beads as our binding targets and APES-coated glass beads as the negative screens during the phage library screening process. After three rounds of screening, 36 of the blue phage plaques containing a single colony were isolated. Figure 5A shows that 26 out of 36 phage colonies display oligopeptide TPFDLRPSSDTR.[38] In the literature, Schonbrunn et al.[39] reported that glyphosate receptors, such as 5-enolpyruvylshikimate-3-phosphate synthase (EPSPS), contains strictly conserved residues of Arg (R)-124, Asp (D)-313, Arg (R)-344, and Arg (R)-386. Binding of glyphosate to these residues can inhibit the EPSPS activity and block the shikimate pathway for synthesis of the aromatic amino acids. Coincidently, our most abundant oligopeptide (TPFDLRPSSDTR), and second most abundant oligopeptide (TDIRLRPLDKRI), also contain two Arg (R) and two Asp (D) residues. Therefore, R and D are probably responsible for the binding of glyphosate through hydrogen bonding and electrostatic interaction. However, more studies and molecular simulations are needed to elucidate the exact binding mechanism of the oligopeptide to glyphosate.

(A)

Phage No.	(N) 1	2	3	4	5	6	7	8	9	10	11	(C) 12	pI	Hydrophobic (%)	Freq.
1	T	P	F	**D**	L	**R**	P	S	S	**D**	T	**R**	6.93	16.67	26/36
2	T	**D**	I	**R**	L	R	P	L	**D**	K	**R**	I	11.22	33.33	4/36
3	R	L	K	P	R	S	D	I	K	P	I	R	12.13	25	1/36
4	S	D	T	P	L	I	K	R	L	D	F	P	6.9	33.33	1/36
5	R	R	S	D	L	K	P	I	R	P	L	K	12.13	25	1/36
6	R	R	K	I	K	P	R	R	R	I	R	P	13.1	16.67	1/36
7	T	R	I	R	P	L	R	R	K	P	I		13.0	25	1/36
8	R	R	I	P	K	L	I	K	R	R	L	R	13.01	33.33	1/36

(B)

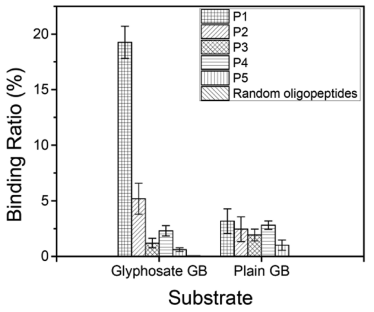

Figure 5. (A) Oligopeptide sequences identified by using phage library screening against glyphosate-functionalized glass beads after 3 rounds. (B) Binding ratio of selected phage colonies to glyphosate-immobilized glass beads and plain glass beads. The phage colonies used in this experiment are isolated single-phage colonies which express oligopeptides, $\mathbf{P_1}$, $\mathbf{P_2}$, $\mathbf{P_3}$, $\mathbf{P_4}$, $\mathbf{P_5}$, or random oligopeptides. The error bar represents a standard deviation of three parallel experiments.

To compare the binding capability and specificity of a phage containing glyphosate-binding oligopeptides, we amplified five single-phage colonies expressing oligopeptide sequences TPFDLRPSSDTR ($\mathbf{P_1}$), TDIRLRPLDKRI ($\mathbf{P_2}$), RLKPRSDIKPIR ($\mathbf{P_3}$), SDTPLIKRLDFP ($\mathbf{P_4}$), and RRSDLKPIRPLK ($\mathbf{P_5}$), to a titering around 10^{12} pfu/mL. Then, these amplified phage colonies together with the original phage library were introduced to glyphosate-immobilized glass beads, respectively. After washing, the bound phage was eluted and titered. The binding ratio is defined as the number of bound phages divided by the number of input phages. Figure 5B shows that the phage colony containing $\mathbf{P_1}$ has the highest binding ratio (19.2%), which is about 2800 times higher than that of the original phage library. The second highest is $\mathbf{P_2}$, which has a binding ratio of 5.2% (800 times higher than that of the original phage library). Interestingly, we notice that both $\mathbf{P_1}$ and $\mathbf{P_2}$ contain a homology tripeptide sequence DXR (X = L,T, I, or K), which is probably responsible for the binding of glyphosate.

For testing their binding specificity, we also introduced phage colonies expressing these oligopeptides to plain glass beads. In this experiment, $\mathbf{P_1}$, $\mathbf{P_2}$, $\mathbf{P_3}$, $\mathbf{P_4}$, and $\mathbf{P_5}$ have similar binding

dx.doi.org/10.1021/ac400273g | Anal. Chem. XXXX, XXX, XXX−XXX

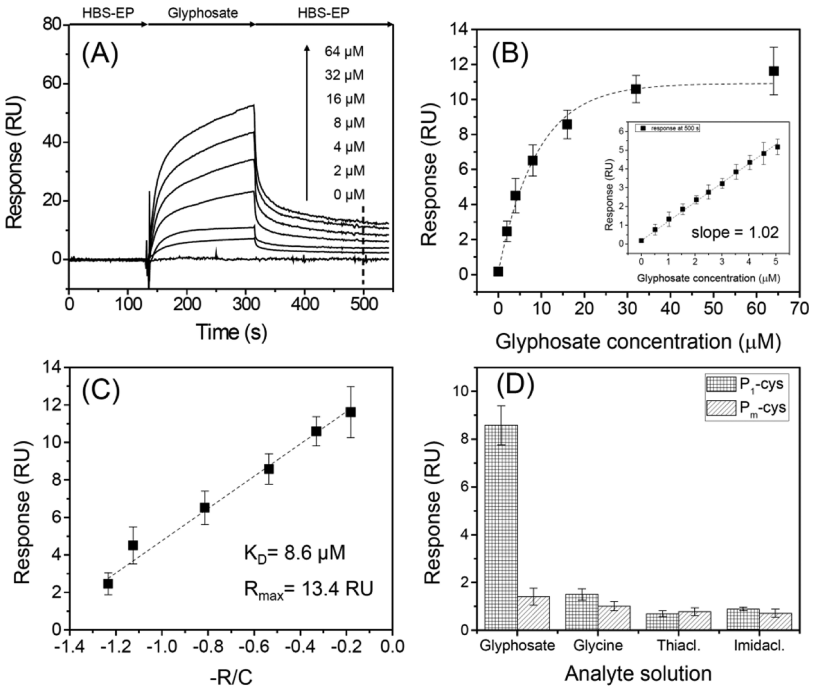

Figure 6. (A) SPR sensorgrams for different concentrations of glyphosate (0, 2, 4, 8, 16, 32, and 64 μM). The sensor chip is modified with $\mathbf{P_1}$-cys with a surface density of 0.6 1/nm^2. (B) SPR responses at various glyphosate concentrations. The inset shows a linear response region when the glyphosate concentration is below 5 μM. (C) Fitting SPR signal response R vs $(-R/C)$ by using the Langmuir isotherm. (D) SPR responses to 16 μM of glyphosate, glycine, thiacloprid, and imidacloprid by using a sensor chip decorated with either $\mathbf{P_1}$-cys or $\mathbf{P_m}$-cys.

ratios, suggesting that the binding to plain glass beads is nonspecific in nature. These results, when combined, suggest that the phage colony containing $\mathbf{P_1}$ has good selectivity to surface-immobilized glyphosate.

SPR Biosensor for Detecting Glyphosate. To detect glyphosate, a SPR gold sensor chip was functionalized with an oligopeptide $\mathbf{P_1}$-cys in situ. After the immobilization, SPR shows an increase of 1659.3 RU, suggesting that oligopeptide is successfully immobilized, and the surface density is 0.6 1/nm^2.[32] To detect glyphosate, HBS-EP buffer containing glyphosate was injected to start a binding cycle which includes a binding step, a rinsing step, and a regeneration step. Sensorgrams at different concentrations of glyphosate in Figure 6A shows that, with increasing concentration of glyphosate, the SPR response increases accordingly. To get the equilibrium binding constants of the oligopeptide receptor to glyphosate, we collected the final SPR response after each binding cycle at 500 s and plotted the final SPR responses against glyphosate concentration.

Figure 6B shows the binding curve of glyphosate from 0 to 64 μM. The inset of Figure 6B shows a linear region of the binding curve between 0 and 5 μM. From the slope of the straight line, we can determine that the sensitivity of the SPR sensor is 1.02 RU/ μM and the limit of detection (LOD) is 0.58 μM.[40] By applying the Langmuir isotherm,[32] the equilibrium dissociation constant (K_D) for glyphosate can be determined to be 8.6 μM by plotting R against $(-R/C)$, where R is the SPR signal response, and C is the corresponding concentration of glyphosate in buffer solution, as shown in Figure 6C.

To identify the role of R and D on the oligopeptide's binding specificity, we replaced R and D residues in $\mathbf{P_1}$-cys with A to obtain an alanine-substituted oligopeptide TPFALAPSSA-TAGGGC ($\mathbf{P_m}$-cys) as control. To compare these two oligopeptides, HBS-EP buffer containing 16 μM of glyphosate was injected into the SPR sensor chip functionalized with $\mathbf{P_1}$-cys or $\mathbf{P_m}$-cys. Figure 6D shows that, when 16 μM of glyphosate solution is injected, the SPR response on $\mathbf{P_m}$-cys functionalized sensor chip is 1.4 RU, which is 6 times lower than that of the sensor chip functionalized with $\mathbf{P_1}$-cys (8.6 RU). To test the binding specificity for glyphosate, buffer solution containing 16 μM glycine, thiacloprid, and imidacloprid are sequentially injected into the SPR sensor chip. Figure 6D shows that the SPR responses for glycine, thiacloprid, and imidacloprid on $\mathbf{P_1}$-cys immobilized sensor chip are only about 1 RU. These results, when combined, suggest that the R and D motifs are responsible for binding glyphosate, and the SPR biosensor functionalized with oligopeptide $\mathbf{P_1}$-cys has good binding specificity toward glyphosate.

Finally, to study the influence of ionic strength and pH on the binding strength, we first prepared HBS-EP buffer containing different concentrations of $MgCl_2$ and 16 μM of glyphosate. Figure 7A shows that the SPR response decreases with increasing Mg^{2+} concentration. This is probably because the strong ionic strength can screen the electrostatic interactions between oligopeptide and glyphosate molecules and reduce the binding strength. Next, to study the influence of pH on the binding strength, we adjusted the pH of the HBS-EP buffer (native pH 7.4) by using hydrochloric acid solution (1 M). Figure 7B shows that the SPR response decreases fast when the pH is below 6.5. We propose that this is because the net charge of oligopeptide (pI = 6.93) changes from negative to positive, and the electrostatic interaction between oligopeptide and glyphosate is affected. This is not surprising because one common method to regenerate the SPR sensor chip (remove the bound molecules) is using low pH solution (such as glycine-HCl, pH 2.0).

dx.doi.org/10.1021/ac400273g | Anal. Chem. XXXX, XXX, XXX−XXX

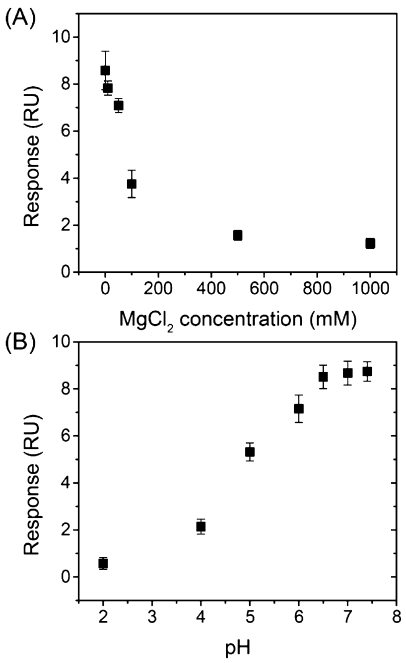

Figure 7. SPR results showing factors that influence the binding strength of oligopeptide to glyphosate. (A) Effect of ionic strength and (B) effect of pH.

CONCLUSIONS

In conclusion, we describe a modified phage display method to enable the biopanning for glyphosate, a highly soluble herbicide. The glyphosate is covalently immobilized on amine-modified glass beads through EDC/NHS chemistry. After three rounds of biopanning, one 12-mer oligopeptide, TPFDLRPSSDTR, was identified from the phage library. The repeatedly and alternately appearing amino acid residues of R and D in the oligopeptide sequence may be responsible for the high binding affinity and specificity. To develop a SPR biosensor for online detection of glyphosate in buffer solution, the modified oligopeptide, TPFDLRPSSDTRGGGC, was immobilized on the gold surface of a SPR sensor chip, and the binding kinetics of glyphosate to oligopeptide were studied. The oligopeptide functionalized SPR biosensor showed good specificity, and the LOD of this biosensor can achieve 0.58 μM.

ASSOCIATED CONTENT

Supporting Information

Additional description on the fluorescence test for binding specificity and conversion of fluorescence intensity into surface density of FITC. This material is available free of charge via the Internet at http://pubs.acs.org.

AUTHOR INFORMATION

Corresponding Author

*Tel.: +65-6516-6614 E-mail: cheyk@nus.edu.sg.

Notes

The authors declare no competing financial interest.

ACKNOWLEDGMENTS

The work was supported by a research scholarship from the National University of Singapore.

REFERENCES

(1) Coutinho, C. F. B.; Coutinho, L. F. M.; Mazo, L. H.; Nixdorf, S. L.; Camara, C. A. P.; Lancas, F. M. *Anal. Chim. Acta* **2007**, *592*, 30−35.
(2) Steinrucken, H. C.; Amrhein, N. *Biochem. Biophys. Res. Commun.* **1980**, *94*, 1207−1212.
(3) Sura, S.; Waiser, M.; Tumber, V.; Lawrence, J. R.; Cessna, A. J.; Glozier, N. *J. Environ. Qual.* **2012**, *41*, 732−743.
(4) Howe, C. M.; Berrill, M.; Pauli, B. D.; Helbing, C. C.; Werry, K.; Veldhoen, N. *Environ. Toxicol. Chem.* **2004**, *23*, 1928−1938.
(5) Gasnier, C.; Dumont, C.; Benachour, N.; Clair, E.; Chagnon, M. C.; Seralini, G. E. *Toxicology* **2009**, *262*, 184−191.
(6) *Drinking Water Standards and Health Advisories*,2011 ed.; United States Environmental Protection Agency (USEPA): Washington, DC, http://water.epa.gov/action/advisories/drinking/upload/dwstandards2012.pdf (accessed on October 13, 2012).
(7) *Guidelines for Canadian Drinking Water Quality Summary Table*; Health Canada: Ottawa, ON, Canada, www.hc-sc.gc.ca/ewh-semt/pubs/water-eau/2012-sum_guide-res_recom/index-eng.php (accessed on October 13, 2012).
(8) Khrolenko, M. V.; Wieczorek, P. P. *J. Chromatogr., A* **2005**, *1093*, 111−117.
(9) Nedelkoska, T. V.; Low, G. K. C. *Anal. Chim. Acta* **2004**, *511*, 145−153.
(10) Saito, T.; Aoki, H.; Namera, A.; Oikawa, H.; Miyazaki, S.; Nakamoto, A.; Inokuchi, S. *Anal. Sci.* **2011**, *27*, 999−1005.
(11) Motojyuku, M.; Saito, T.; Akieda, K.; Otsuka, H.; Yamamoto, I.; Inokuchi, S. *J. Chromatogr., B* **2008**, *875*, 509−514.
(12) Sancho, J. V.; Hernandez, F.; Lopez, F. J.; Hogendoorn, E. A.; Dijkman, E.; vanZoonen, P. *J. Chromatogr., A* **1996**, *737*, 75−83.
(13) Abdullah, M. P.; Daud, J.; Hong, K. S.; Yew, C. H. *J. Chromatogr., A* **1995**, *697*, 363−369.
(14) Coutinho, C. F. B.; Coutinho, L. F. M.; Mazo, L. H.; Nixdorf, S. L.; Camara, C. A. P. *J. Chromatogr., A* **2008**, *1208*, 246−249.
(15) Soga, T.; Imaizumi, M. *Electrophoresis* **2001**, *22*, 3418−3425.
(16) Goodwin, L.; Startin, J. R.; Keely, B. J.; Goodall, D. M. *J. Chromatogr., A* **2003**, *1004*, 107−119.
(17) Sanchez-Bayo, F.; Hyne, R. V.; Desseille, K. L. *Anal. Chim. Acta* **2010**, *675*, 125−131.
(18) Songa, E. A.; Arotiba, O. A.; Owino, J. H. O.; Jahed, N.; Baker, P. G. L.; Iwuoha, E. I. *Bioelectrochemistry* **2009**, *75*, 117−123.
(19) Clegg, B. S.; Stephenson, G. R.; Hall, J. C. *J. Agric. Food. Chem.* **1999**, *47*, 5031−5037.
(20) Rubio, F.; Veldhuis, L. J.; Clegg, B. S.; Fleeker, J. R.; Hall, J. C. *J. Agric. Food. Chem.* **2003**, *51*, 691−696.
(21) Dover, J. E.; Hwang, G. M.; Mullen, E. H.; Prorok, B. C.; Suh, S. J. *J. Microbiol. Methods* **2009**, *78*, 10−19.
(22) Iqbal, S. S.; Mayo, M. W.; Bruno, J. G.; Bronk, B. V.; Batt, C. A.; Chambers, J. P. *Biosens. Bioelectron.* **2000**, *15*, 549−578.
(23) Brigati, J. R.; Petrenko, V. A. *Anal. Bioanal. Chem.* **2005**, *382*, 1346−1350.
(24) Bi, X. Y.; Yang, K. L. *Biosens. Bioelectron.* **2010**, *26*, 107−111.
(25) Kim, M. Y.; Kim, O. R.; Choi, Y. S.; Lee, H.; Park, K.; Lee, C. T.; Kang, K. W.; Jeong, S. *Mol. Cells* **2012**, *33*, 71−77.
(26) Lee, S. W.; Mao, C. B.; Flynn, C. E.; Belcher, A. M. *Science* **2002**, *296*, 892−895.
(27) Flynn, C. E.; Mao, C. B.; Hayhurst, A.; Williams, J. L.; Georgiou, G.; Iverson, B.; Belcher, A. M. *J. Mater. Chem.* **2003**, *13*, 2414−2421.
(28) Rothenstein, D.; Claasen, B.; Omiecienski, B.; Lammel, P.; Bill, J. *J. Am. Chem. Soc.* **2012**, *134*, 12547−12556.
(29) Chen, H. B.; Su, X. D.; Neoh, K. G.; Choe, W. S. *Anal. Chem.* **2006**, *78*, 4872−4879.
(30) Jaworski, J. W.; Raorane, D.; Huh, J. H.; Majumdar, A.; Lee, S. W. *Langmuir* **2008**, *24*, 4938−4943.
(31) Cerruti, M.; Jaworski, J.; Raorane, D.; Zueger, C.; Varadarajan, J.; Carraro, C.; Lee, S. W.; Maboudian, R.; Majumdar, A. *Anal. Chem.* **2009**, *81*, 4192−4199.
(32) Ding, X. K.; Zhang, W.; Cheng, D.; He, J. Z.; Yang, K. L. *Biosens. Bioelectron.* **2012**, *35*, 271−276.

(33) Cho, W. R.; Fowler, J. D.; Furst, E. M. *Langmuir* **2012**, *28*, 6013−6020.
(34) Cui, Y.; Pattabiraman, A.; Lisko, B.; Collins, S. C.; McAlpine, M. C. *J. Am. Chem. Soc.* **2010**, *132*, 1204−1205.
(35) *New England Biolab Phage Display Manual*; https://www.neb.com/ (accessed on March 07, 2013).
(36) Yang, C. Y.; Brooks, E.; Li, Y.; Denny, P.; Ho, C. M.; Qi, F. X.; Shi, W. Y.; Wolinsky, L.; Wu, B.; Wong, D. T. W.; Montemagno, C. D. *Lab Chip* **2005**, *5*, 1017−1023.
(37) Moon, J. H.; Shin, J. W.; Kim, S. Y.; Park, J. W. *Langmuir* **1996**, *12*, 4621−4624.
(38) The iso-electric point (p*I*) and hydrophobic percentages were calculated from an online peptide calculator http://www.innovagen.se/custom-peptide-synthesis/peptide-property-calculator/peptide-property-calculator.asp (accessed on October 14, 2012).
(39) Schonbrunn, E.; Eschenburg, S.; Shuttleworth, W. A.; Schloss, J. V.; Amrhein, N.; Evans, J. N. S.; Kabsch, W. *Proc. Natl. Acad. Sci. U.S.A.* **2001**, *98*, 1376−1380.
(40) Hwang, K. S.; Lee, M. H.; Lee, J.; Yeo, W. S.; Lee, J. N.; Kim, K. M.; Kang, J. Y.; Kim, T. S. *Biosens. Bioelectron.* **2011**, *30*, 249−254.

dx.doi.org/10.1021/ac400273g | *Anal. Chem.* XXXX, XXX, XXX−XXX